A time-domain approach to predict sound radiation from track vibrations

25·29 August 2024
inter.noise
NANTES FRANCE

A time-domain approach to predict sound radiation from track vibrations

Jannik Theyssen[1]
Division of Applied Acoustics, Department of Architecture and Civil Engineering
Chalmers University of Technology, 412 96 Gothenburg, Sweden

Jens C. O. Nielsen[2]
Division of Dynamics, Department of Mechanics and Maritime Sciences
Chalmers University of Technology, 412 96 Gothenburg, Sweden

Astrid Pieringer[3]
Division of Applied Acoustics, Department of Architecture and Civil Engineering
Chalmers University of Technology, 412 96 Gothenburg, Sweden

ABSTRACT

With the intended shift of transport from road to railway, noise exposure due to railway noise will increase. Auralisation of the noise is a key tool for assessing noise perception beyond equivalent sound pressure levels. Researching the connection between, for example, track design parameters and perceived sound quality holds potential for perception-centered track design. A computationally efficient model is required to render the sound field generated by the track vibration. In this paper, using simulated time-domain surface velocities of a rail and sleepers as input, such a model is presented. The sound pressure signal in a position on the side of the track is efficiently predicted by convolving these velocities with precalculated acoustic transfer functions. For a typical ballasted track, the necessary spatial discretisation of the evaluated velocities is determined in a convergence study. Further, the required length of the finite section of the track to be included in the prediction is specified. Finally, pass-by signals generated by track vibration are demonstrated.

1. INTRODUCTION

Shifting freight and passenger transport from road to rail will also shift some of the traffic noise exposure from road to rail. Therefore, railway noise mitigation measures are being implemented in several countries. However, noise mitigation measures should not undermine the competitiveness of railway transport, being a sustainable way of transport and a key to achieving climate goals [1]. It is essential that the way railway noise is quantified correlates with the effect on human health and human perception. The latter has two aspects: Perceived annoyance should correlate with the way the noise is described, and the descriptors should facilitate communication about the noise.

[1]jannik.theyssen@chalmers.se

[2]jens.nielsen@chalmers.se

[3]astrid.pieringer@chalmers.se

Auralisation of railway noise can be a tool to not only assess human noise perception, but also to aid communication about the noise with various interest groups. In contrast to the commonly used equivalent levels, an auralisation can produce an intuitive understanding of the noise. For example, the effect of transient noise emerging due to wheel-rail impacts generated by wheel flats or at railway crossings may not be adequately described by the equivalent levels. As the track is one of the main sources of railway rolling noise, this paper focusses on the radiation from vertical vibration of the track.

One approach to auralise rail vibrations is based on distributing equivalent sources, such as monopoles, in the longitudinal direction of the track. Pieren et al. [2], inspired by CNOSSOS [3], include one monopole source per wheel for the track vibration. A recent study [4] that applies auralisation to evaluate acoustic pleasentness of railway noise uses a similar approach. Maillard et al. [5] use a line of equidistant, coherent monopoles along the rail. The monopoles are spaced with a fraction, e.g., 1/5, of the shortest wavelength in the air and the structure. The attenuation of the structural response determines the total number of sources.

In this work, a simulation tool for vertical vibrations of railway track is combined with an efficient model of sound radiation, with the aim of optimising track design with a focus on human perception. A high temporal and spatial resolution is necessary to efficiently auralise noise radiated from railway tracks. To address this and reduce the computational cost, the presented model uses precalculated acoustic transfer functions. In contrast to the method [6, 7] presented in earlier work by the authors, here impulse responses are used to describe the pressure in a trackside position for a given rail velocity distribution in a short section of the rail. Convolution of these impulse responses with the rail and sleeper velocity produces the pass-by sound pressure. The presented method uses the Wavenumber domain Boundary Element method (2.5D BE) to calculate the impulse responses from a number of sections on the rail and the sleepers.

This paper addresses the demands regarding the length of each rail section and the required total length of the track model. In contrast to methods based on equivalent roughness spectra like TWINS [8] or SILVARSTAR [9], this approach predicts the rolling contact forces, track vibration, and sound pressure levels in the time domain and is thus fit to be used for, for example, auralising transients in the rolling contact forces.

2. METHOD

A discretely supported 60E1 rail is modelled by Rayleigh-Timoshenko beam finite elements in the in-house software DIFF [11]. The principle setup is presented in Figure 1 and the corresponding parameters are described in Table 1. The sleepers are modelled as rigid masses. A single wheel pass-by is simulated with a simplified wheelset model with two degrees of freedom: The wheel with radius 0.45 m and mass m_w is supported by the primary suspension stiffness k_w and primary suspension damping c_w. The mass m_w is also connected to a small mass m'_w via the stiffness k'_w and damper c'_w. The input data to m'_w, k'_w and c'_w are tuned to match the average receptance from a finite element model of the wheel [10, 12]. A total of 300 sleepers are included in the model, distributed with 0.6 m equidistant sleeper spacing. To reduce the time for the simulation of vertical dynamic vehicle-track interaction, the track model is taken as linear and a complex-valued modal approach with a truncated mode set is applied. In this paper, 1250 mode pairs with eigenfrequencies reaching up to 5 kHz are considered.

Time-domain simulations are carried out with one wheel passing over one rail. The rail roughness is based on a measured roughness from the iron ore line in northern Sweden [13], while the wheel roughness is based on a wheel with sinter brake blocks [14]. The vehicle speed is $v = 200$ km/h, and the static preload is $F_p = 54$ kN. The simulation is carried out at a sampling rate of 10 kHz. In a post-processing step, the calculated vertical rail and sleeper velocities are stored for each time step. The spatial resolution of the evaluation points along the rail is 32 sampling points per sleeper bay. Rail velocities at positions between and including sleepers 100 and 200 are

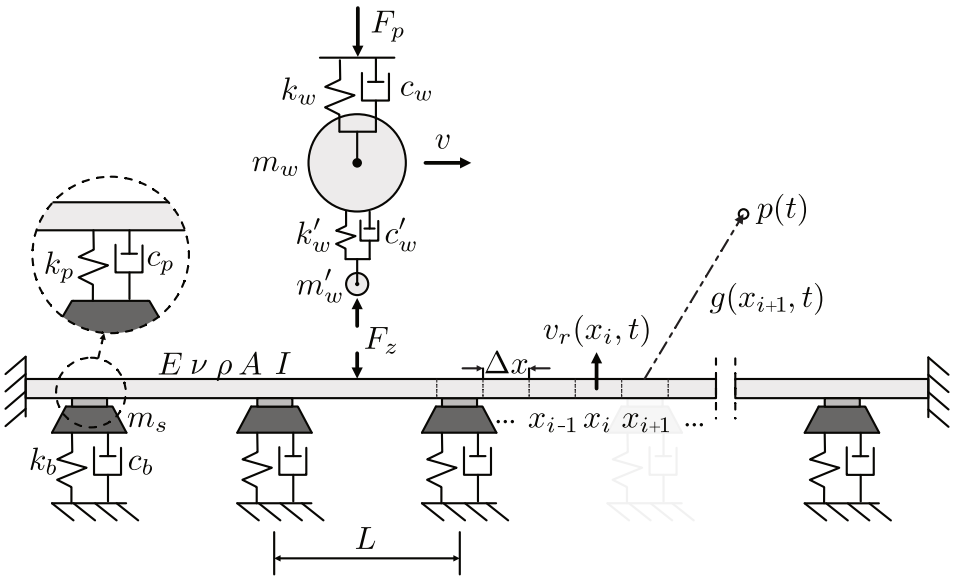

Figure 1: Sketch of dynamic vehicle–track interaction model in DIFF (based on [10]), and discretisation of the rail for the calculation of pass-by sound pressure.

exported from DIFF. The position of sleeper 150 in the centre of this section is defined as $x = 0$ m.

Precalculated acoustic transfer functions are used to predict the sound radiation. The transfer functions evaluated using a 2.5D BE model allow for a complex 2D geometry of the cross-section, while assuming a constant cross-section along the third dimension. Here, these transfer functions are transformed to the time and space domains and used as Green's functions $g(t,x)$, as briefly discussed in the following paragraphs.

The transfer function $G(\omega,\kappa)$ describes the pressure in a track-side position for a unit normal velocity on the rail surface in the wavenumber-frequency domain [6]. Theyssen et al. [15] presented a method to generate such transfer functions for arbirary wavenumber spectra given acoustically hard geometries. This method facilitates creating transfer functions with the high spatial resolution necessary for an auralisation.

The 2D inverse Fourier transform of $G(\omega,\kappa)$,

$$g(t,x) = \frac{1}{4\pi^2}\int_{-\infty}^{\infty}\int_{-\infty}^{\infty} G(\omega,\kappa)\mathrm{e}^{i(\omega t-\kappa x)}\mathrm{d}\omega\mathrm{d}\kappa \tag{1}$$

produces impulse responses that describe the sound pressure signal along the track for a unit velocity pulse at $x = 0$ m. The maximum wavenumber in the wavenumber spectrum is chosen based on the discretisation of the exported rail velocities. As the acoustic geometry is constant along the rail, the generated impulse responses can be used to describe the pressure signal at $x = 0$ m for a given velocity $v_r(x,t)$ along the rail.

The pressure signal generated by the rail vibration is then calculated by convolution of the rail velocity $v_r(x,t)$ with $g(x,t)$,

$$p(t) = \int_{x=-\infty}^{\infty}\int_{\tau=0}^{t} v_r(x,\tau)g(x,t-\tau)\mathrm{d}\tau\mathrm{d}x \tag{2}$$

In practise, only a finite length L of the rail vibration produces significant sound pressure at the listener position $x = 0$ m. Further, given the necessary spatial discretisation of the rail velocity export, only a finite number of rail sections N_x of length Δx need to be included in the calculation (cf. Fig. 1). The discrete formulation of the convolution becomes

$$p(t_i) = \sum_{x_i=0}^{N_x-1}\sum_{t_i=0}^{N_t-1} v_r(x_i,t_i)g(x_i,N_t-t_i)\Delta x\Delta t \tag{3}$$

Table 1: Simulation parameters

Wheel mass	m_w	519.75	kg
Primary suspension stiffness	k_w	1.31	MN/m
Primary suspension damping	c_w	11.16	kNs/m
Extra stiffness	k'_w	6220	MN/m
Small mass	m'_w	3	kg
Extra damping	c'_w	23.2	kNs/m
Rail Young's modulus	E	210	GPa
Rail Poisson's ratio	ν	0.3	-
Rail density	ρ	7850	kg/m^3
Rail cross-sectional area	A	7.643e-3	m^2
Second moment of inertia	I	3.022e-5	m^4
Rail pad stiffness	k_p	114	MN/m
Rail pad damping	c_p	5	kNs/mm
Sleeper mass	m_s	140	kg
Ballast stiffness per half sleeper	k_b	75	MN/m
Ballast damping per half sleeper	c_b	150	MN/m

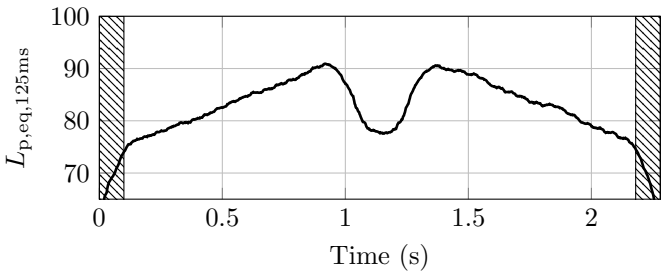

Figure 2: Short-term equivalent sound pressure level at 7.5 m from the track centre, 1.2 m above the rail, next to sleeper 150, produced by the vertical rail vibration.

with the time increment Δt and the number N_t of time samples in the velocity export.

3. RESULTS

This section presents a typical result and discusses the necessary spatial resolution of the rail velocity export and the necessary total length of the rail. Figure 2 presents the short-term equivalent sound pressure level at the receiver position 1.2 m above the rail, 7.5 m from the centre of the track. Of the two rails, only the one closer to the receiver position is considered. Short-term equivalent levels of up to 90 dB are observed. A distinct dip is visible when the wheel is closest to the receiver position. This effect is due to bending waves in the rail radiating airborne sound at an angle depending on the wavelengths in the structure and air. The radiation from the rail towards the receiver is highest when the wheel is located at some distance before and after $x = 0$. The shaded edges of the figure mark invalid sections of the results produced due to zero-padding in the convolution. These signals are omitted from further calculations.

For the following convergence studies, a coefficient C is introduced to quantify the similarity

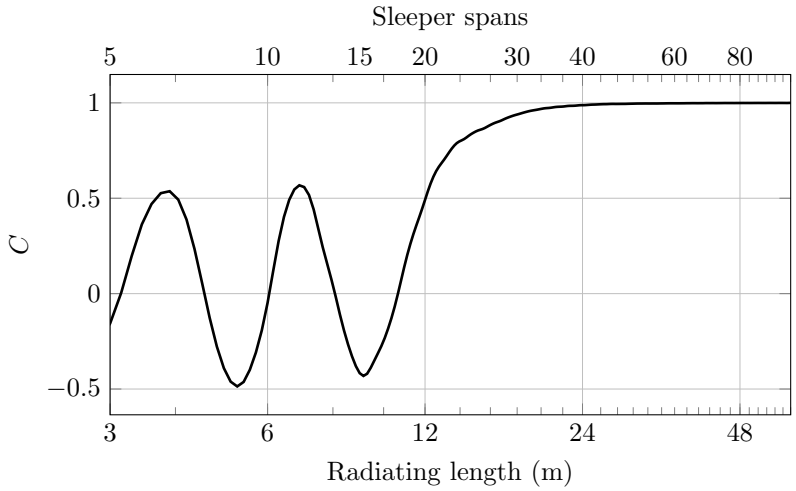

Figure 3: Convergence of the sound pressure signal for increasing length of the considered radiating section of the rail.

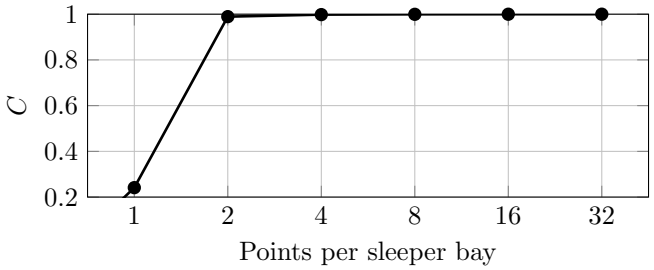

Figure 4: Convergence of the sound pressure signal for different number of points per sleeper bay.

of two signals,

$$C(\mathbf{p}, \mathbf{p}_{\text{ref}}) = \frac{\mathbf{p} \cdot \mathbf{p}_{\text{ref}}^T}{|\mathbf{p}_{\text{ref}}|^2} \tag{4}$$

where the time signals are compared using their dot products and scaled with the squared norm of the reference signal. This produces a unit coefficient for identical signals.

Figure 3 shows the convergence of the coefficient C for an increasing total length L of the rail included in the prediction of the pressure signal. Only the total number of points is varied, the track model used for the prediction of the velocity is not altered. The length L is adjusted so that the receiver position is always centred with L/2 on either side of $x = 0$. It is clear that beyond a certain length, the rail vibration at the edges of this length does not contribute significantly to the sound pressure at the centre and can be omitted for sound prediction. For the chosen track configuration, this length is about 24 m or about 40 sleeper spans, where a coefficient $C > 0.99$ is reached.

To investigate the necessary spatial discretisation, the pressure signal is first predicted with a discretisation of 32 points per sleeper span, or $\Delta x = 18.75$ mm. The total length of the radiating rail is 100 sleeper spans or 60 m. The pressure signals produced with other discretisations are then compared to this reference signal p_{ref}. Figure 4 shows the convergence of the pressure signal for different numbers of points per sleeper bay. It is clear that the signals produced with two points per sleeper bay and higher are very similar to those produced with 32 points per sleeper bay.

This spatial discretisation is lower compared to alternative approaches with usual equivalent sources such as low-order multipoles. The spacing of such multipoles needs to be dense enough to avoid spatial aliasing and is thus determined by the wavelength in air. However, in this case, the generated impulse responses already contain the information about the spatial extent of the

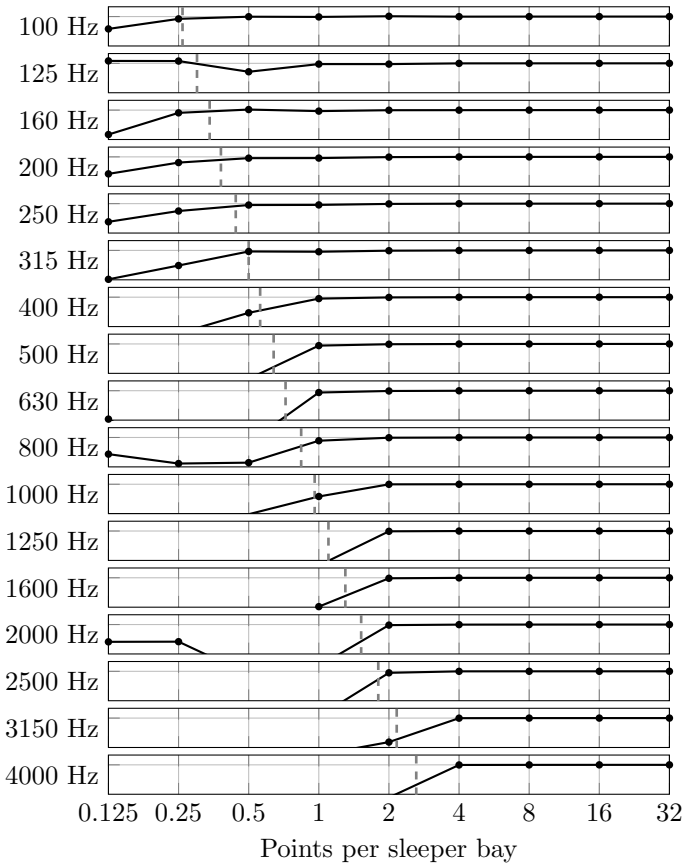

Figure 5: Convergence C for third-octave band filtered pressure signals. The vertical, dashed lines indicate half a wavelength of vertical bending waves at the centre frequency of each band.

source. For illustration, in the extreme case of $\Delta x = L$, one impulse response would suffice to describe the signal produced by the rigid body motion of the rail. The required spatial resolution is therefore only a consequence of the shortest bending wavelength in the rail. An analysis of this convergence for different third-octave bands shows this dependency. Figure 5 shows the convergence in 17 third-octave bands. Half the wavelength of vertical bending waves in the rail, at the centre frequency of each band, is indicated with vertical dashed lines. It is clear that the spatial discretisation is high enough when more than two points per bending wavelength are included in the prediction. The fact that the convergence of the total signal converges at two points per sleeper bay as shown in Figure 4 indicates that the velocity spectrum for the given load case does not contain relevant information at shorter wavelengths, i.e. in the frequency range above 3.15 kHz and upwards. The reason for this is the studied combination of vehicle speed, combined wheel and rail roughnessand track model. It can be shown that for an uncorrelated distribution of vibration velocity in 32 discrete points per sleeper bay, all 32 points per sleeper bay are necessary to produce a coefficient $C = 1$.

The computation time for calculating the discussed signals is comparatively short, given that the prediction is based on physical models. The computation time to predict the sound pressure signal for a model length of 100 sleeper spans with 8 velocity points per span and a total simulation length of 27000 time samples (corresponding to 2.7 seconds of wheel motion at 10 kHz sampling frequency) is about 8.4 seconds. The calculations were carried out on an Apple M2 Pro laptop computer and include loading and generating the acoustic transfer functions in time and space domains, loading the rail velocity data, the convolution, and storing the results. The acoustic transfer functions can be stored and reused for different velocity inputs.

4. CONCLUSIONS

A simulation approach for calculating time-domain sound pressure signals due to vertical rail vibration has been presented. The approach is computationally very efficient as a result of the use of precalculated acoustic transfer functions. The discretisation and length of the rail section necessary for the prediction of the sound pressure signal has been investigated in a convergence study. It is found that, for the given track and roughness parameters, a finite track section of about 25 m is sufficient for simulating the sound pressure signal created by vertical rail vibrations at a track-side receiver at the position 7.5 m from the track centre, 1.2 m above the rail head. Furthermore, a spatial discretisation of two nodes per sleeper bay was found to be sufficient for the given rail velocity distribution. However, other roughness excitation spectra and/or track models can produce velocity distributions on the rail that require higher spatial resolutions. The computation times for the post-processing of the pressure signals were found to be in the order of a few seconds. This modelling approach enables efficient studies of noise radiation from railway track and can be used by other researchers with access to simulated rail vibration data in the time domain.

ACKNOWLEDGEMENTS

The current study is part of the ongoing activities in CHARMEC - Chalmers Railway Mechanics (www.charmec.chalmers.se). This work is financed by Chalmers University of Technology, Transport Area of Advance/SFO Transport.

REFERENCES

1. Jakob Oertli. Railway noise mitigation framework in Europe: Combining policies with the concerns of the railways. In Geert Degrande, Geert Lombaert, David Anderson, Paul de Vos, Pierre-Etienne Gautier, Masanobu Iida, James Tuman Nelson, Jens C. O. Nielsen, David J. Thompson, Thorsten Tielkes, and David A. Towers, editors, *Noise and Vibration Mitigation for Rail Transportation Systems*, volume 150, pages 197–205. Springer International Publishing, Cham, 2021. Notes on Numerical Fluid Mechanics and Multidisciplinary Design.
2. Reto Pieren, Kurt Heutschi, Jean Marc Wunderli, Mirjam Snellen, and Dick G. Simons. Auralization of railway noise: Emission synthesis of rolling and impact noise. *Applied Acoustics*, 127:34–45, 2017.
3. European Commission. Joint Research Centre. ICHP. *Common noise assessment methods in Europe (CNOSSOS-EU): to be used by the EU member states for strategic noise mapping following adoption as specified in the environmental noise directive 2002/49/EC.* Publications Office, 2012.
4. Sarah Weidenfeld, Marie-Therese Schmitz, Sandra Sanok, Arne Henning, Daniel Aeschbach, and Eva-Maria Elmenhorst. Effects of railway rolling noise on perceived pleasantness. *Transportation Research Part D: Transport and Environment*, 126:103995, 2024.
5. Julien Maillard, Abbès Kacem, Nadine Martin, and Baldrik Faure. Physically-based auralization of railway rolling noise. In *Proceedings of the 23rd International Congress on Acoustics*, pages 1667–1674, Aachen, 2019. Deutsche Gesellschaft für Akustik e.V. (DEGA).
6. Jannik Theyssen. Towards time-domain modelling of wheel/rail noise: Effect of the dynamic track model. *Proceedings of the Institution of Mechanical Engineers, Part F: Journal of Rail and Rapid Transit*, 238(4):350–359, 2024.
7. Jannik Theyssen, Astrid Pieringer, and Wolfgang Kropp. Optimizing components in the rail support system for dynamic vibration absorption and pass-by noise reduction. In Xiaozhen Sheng, David Thompson, Geert Degrande, Jens C. O. Nielsen, Pierre-Etienne Gautier, Kiyoshi Nagakura, Ard Kuijpers, James Tuman Nelson, David A. Towers, David Anderson, and Thorsten

Tielkes, editors, *Noise and Vibration Mitigation for Rail Transportation Systems*, Lecture Notes in Mechanical Engineering, pages 673–681, Singapore, 2024. Springer Nature.

8. David Thompson, Brian Hemsworth, and Nicolas Vincent. Experimental validation of the TWINS prediction program for rolling noise, part 1: Description of the model and method. *Journal of Sound and Vibration*, 193(1):123–135, 1996.
9. Reto Pieren, Fotis Georgiou, Giacomo Squicciarini, Kurt Heutschi, and David Thompson. VR demonstration of railway noise mitigation using auralised train pass-bys. In *Proceedings of the 10th Convention of the European Acoustics Association Forum Acusticum 2023*, pages 5629–5635, Turin, Italy, 2024. European Acoustics Association.
10. Jens C. O. Nielsen. High-frequency vertical wheel–rail contact forces—Validation of a prediction model by field testing. *Wear*, 265(9-10):1465–1471, 2008.
11. Jens C. O. Nielsen and Annika Igeland. Vertical dynamic interaction between train and track influence of wheel and track imperfections. *Journal of Sound and Vibration*, 187:825–839, 1995.
12. Astrid Pieringer and Wolfgang Kropp. Model-based estimation of rail roughness from axle box acceleration. *Applied Acoustics*, 193:108760, 2022.
13. Jannik Theyssen and Astrid Pieringer. Comparative rolling noise measurements on two railway track types in northern Sweden. Technical report, Chalmers University of Technology, 2024.
14. David J. Thompson and Paul J. Remington. The effects of transverse profile on the excitation of wheel/rail noise. *Journal of Sound and Vibration*, 231(3):537–548, 2000.
15. Jannik Theyssen, Astrid Pieringer, and Wolfgang Kropp. Efficient calculation of the three-dimensional sound pressure field around a slab track. *Acta Acustica*, 8:4, 2024.